Analytical method for forces between current carrying infinite bars

Analytical method for forces between current carrying infinite bars

This paper adds a new compact expression for the forces between straight non-adjacent rectangular conductors with different cross sections and the result can be considered as a new tool as holds for all the analytical expression found in the literature.

II. Previous work

With the laws of Ampère and Lorentz one obtains easily the force between two parallel current carrying conductors with infinite length. But the influence of the conductor cross section cannot always be neglected and one gets a surprising result even for two round wires as shown in the Appendix 1.

The first expression found giving the force per unit length between two infinitely long rectangular conductors is given in (Dwight, 1917). The cross section of the conductors is given by $2a$ and $2b$ with x as the center to center distance in the x direction. A condensed form of this expression is:

$$F_x(x,a,b) = \frac{\mu_0 J_1 J_2}{4\pi}\left[\sum_{i=-1,0,1}\left(4b\left(p_i^2-\frac{4b^2}{3}\right)\arctan\left(\frac{2b}{p_i}\right)+p_i\left(4b^2-\frac{p_i^2}{3}\right)\log\left(\frac{p_i^2+4b^2}{x^2}\right)\right)(|i|-2)(-1)^i+\frac{2}{3}\sum_{j=0}^{1}q_j^3\log\left(\frac{q_j}{x}\right)\right], \tag{1}$$

with $p_i = x + 2\,i\,a$ and $q_j = x + (-1)^j a$.

The existence of busbar systems for power delivery with two parallel 3-phase systems, with the second system above the first one was for the second author the reason to search for an analytical equation allowing also a displacement in the y-direction, leading to (Canova and Giaccone, 2009). During this work the authors realized that the analytical equations provided in (Canova and Giaccone, 2009) are affected by some typographical mistakes. Therefore, the corrections summarized in Appendix 2, or given more detailed in (Giaccone and Canova, 2014), are needed to properly compare the methodology proposed in the present work. The results of (Dwight, 1917). and (Canova and Giaccone, 2009) will be used as verification of the new equations.

III. Model description and solution

Fig. 1 gives the principal geometry of two parallel bars having

- a uniform current density of J_1 and J_2,
- the cross section $2a\times 2b$ and $2A\times 2B$,
- an infinite length in the z-direction and
- the relative position of the bar gravity centers x, y.

To be determined are the forces F_x and F_y. The equation to be evaluated is:

$$\boldsymbol{F} = \iiint\limits_{Vol_2} \boldsymbol{J}_2 \times \boldsymbol{B}\, dV = \iiint\limits_{Vol_2} \begin{bmatrix} -J_2 B_y(J_1, x', y', a, b) \\ J_2 B_x(J_1, x', y', a, b) \\ 0 \end{bmatrix} dV. \tag{2}$$

F is the total force acting on the second conductors and ***B*** is the magnetic flux density with B_x and B_y as its components. The value of B_z is equal to zero because J_2 flows in the *z*-direction. x' and y' are the variable of integration that define the position of the integration point inside the second conductor.

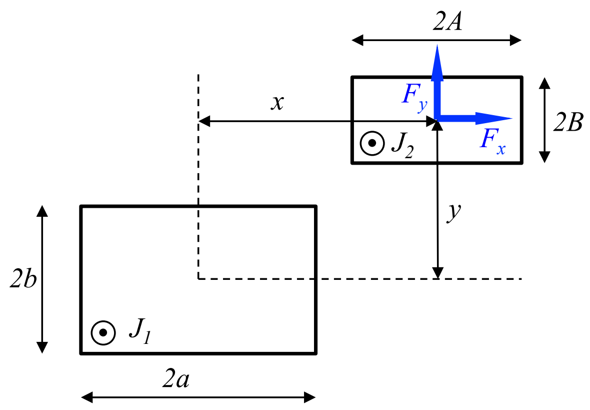

Fig. 1, cross-sections of two massive conductors.

Defining S_2 as the cross-section of the second conductor, one obtains as force per unit length in the z-direction:

$$\begin{bmatrix} F_x \\ F_y \\ F_z \end{bmatrix} = \int\limits_{x-A}^{x+A} \int\limits_{y-B}^{y+B} \begin{bmatrix} -J_2 B_y(J_1, x', y', a, b) \\ J_2 B_x(J_1, x', y', a, b) \\ 0 \end{bmatrix} dS_2. \tag{3}$$

Many ways can be followed to obtain the magnetic flux density as e.g. given by (Pissanetzky, 1990). Here we follow the path via the magnetic vector potential ***A*** due to current J_1. (Urankar, 1982) gives this potential, having a *z*-component only, as:

$$A_z(J_1, x', y', a, b) = \frac{\mu_0 J_1}{16\, ab\pi} \sum_{i=0}^{1} \sum_{j=0}^{1} u_i v_j \log\left(u_i^2 + v_j^2\right) + u_i^2 \arctan\left(\frac{v_j}{u_i}\right) + v_j^2 \arctan\left(\frac{u_i}{v_j}\right) \tag{4}$$

with $u_i = a - (-1)^i x'$ and $v_j = b - (-1)^j y'$. The background of the vector potential is described in (Hammond, 2015).

The magnetic flux density is obtained as:

$$\boldsymbol{B}(\boldsymbol{J}_1, x', y', a, b) = curl[\boldsymbol{A}] = \begin{bmatrix} {\partial A_z}/{\partial y} \\ -{\partial A_z}/{\partial x} \\ 0 \end{bmatrix} \tag{5}$$

The attention will be given now only to the force component F_x because, by using a coordinate rotation, one gets easily the component F_y using the results of F_x. One needs B_y according to eq. (3) and obtains this via eq. (5) :

$$B_y(J, x', y', a, b) = \frac{\mu_0 J_1}{2\pi} \sum_{i=0}^{1} \sum_{j=0}^{1} (-1)^{i+j} \left\{ p_i \arctan\left(\frac{q_j}{p_i}\right) + \frac{q_j}{2} \log\left(p_i^2 + q_j^2\right) \right\} \tag{6}$$

with $p_i = x' + (-1)^i a$ and $q_j = y' + (-1)^j b$.

The definition of:

$$f_x(J_1, J_2, x', y', a, b) = \iint -J_2 B_y(J_1, x', y', a, b) dy'\, dx' \tag{7}$$

and the substitution of eq. (6) leads to:

$$f_x(J_1, J_2, x', y', a, b) = \iint -J_2 \frac{\mu_0 J_1}{2\pi} \sum_{i=0}^{1} \sum_{j=0}^{1} (-1)^{i+j} \left\{ p_i \arctan\left(\frac{q_j}{p_i}\right) + \frac{q_j}{2} \log\left(p_i^2 + q_j^2\right) \right\} dy'\, dx' \tag{8}$$

The results of this double integration with the symbolic solver of Mathematica (Wolfram, 2012) are manually reduced to:

$$f_x(J_1, J_2, x', y', a, b) = \frac{\mu_0 J_1 J_2}{24\pi} \left[\sum_{i=0}^{1} \sum_{j=0}^{1} (-1)^j \left\{ r_i\left(3s_j^2 - r_i^2\right) \log\left(r_i^2 + s_j^2\right) + 2s_j\left(3r_i^2 - s_j^2\right) \arctan\left(\frac{s_j}{r_i}\right) \right\} \right] \tag{9}$$

with $r_\mathrm{i} = a + (-1)^\mathrm{i} x'$ and $s_j = b + (-1)^j y'$.

Subsequently one must substitute the lower and upper boundaries of the integration to get the force, according:

$$\begin{aligned} F_x(J_1, J_2, x, y, a, b, A, B) &= f_x(J_1, J_2, x', y', a, b)\Big|_{x'=x-A}^{x+A}\Big|_{y'=y-B}^{y+B} \\ &= \sum_{p=0}^{1} \sum_{q=0}^{1} (-1)^{p+q} f_x(J_1, J_2, x + (-1)^p A, y + (-1)^q B, a, b). \end{aligned} \tag{10}$$

Eq. (9) and eq. (10) are the solution for the *x*-force per unit length. As described earlier, the *y*-force can be obtained using the F_x equation. Considering a 90° rotation of Fig. 1 as shown in Fig. 2, all the geometrical quantities as well as the forces modify their orientation. The dimensions a, A and the displacement x are now aligned to the y direction. Conversely, the dimensions b, B and the y displacement are aligned with the x-axis. Bearing all this in mind, it is apparent that the y-force represented in Fig. 1 and redrawn in Fig.2 is equal and opposite to the x-force computed according to Fig. 2. In the end, one can compute F_y as:

$$F_y(J_1, J_2, x, y, a, b, A, B) = -F_x(J_1, J_2, -y, x, b, a, B, A). \quad (11)$$

The same relation can be also expressed as:

$$F_y(J_1, J_2, x, y, a, b, A, B) = F_x(J_1, J_2, y, x, b, a, B, A). \quad (12)$$

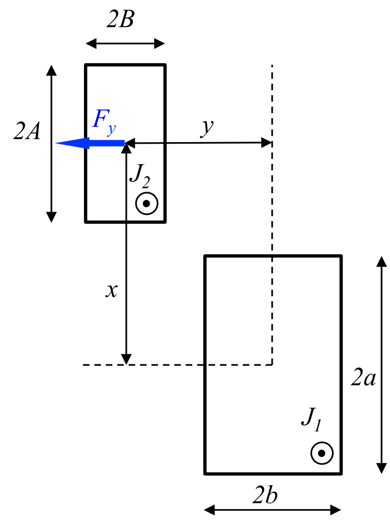

Fig. 2, 90° rotation of the geometry represented in Fig. 1.

IV. SOLUTION VERIFICATION

A comparison with three other methods will be described to ensure validity of the developed equations.

A. Comparison with eq. (1)

In the first verification we compare the results with eq. (1). The same cross-section for both conductors has to be applied consequently. The relative deviation between eq. (1) versus eq. (9) and (10) is analyzed with $a = A = 0.01$ m, $J_1 = J_2 = 10^7 \mathrm{A/m^2}$, $b = B = 0.001 \cdots 0.1$ m and a displacement $x = 0.02 \cdots 0.1\ m$. The relative deviation is $1 - F_{eq_1}/F_{eq_{10}}$ is shown in Fig. 3 and confirms agreement.

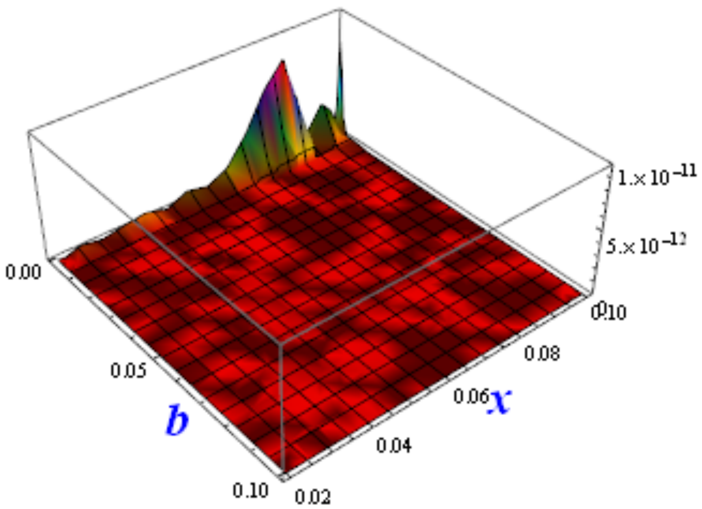

Fig. 3, relative deviation eq. (1) versus eq. (10).

B. Comparison with numerical integration

In the second verification we compared eq. (10) with the numerical integration of eq. (8) considering $a = 0.01$ m, $A = 0.01$ m, $b = 0.04$ m, $B = 0.01$ m, $J_1 = J_2 = 10^7 \mathrm{A/m^2}$. We investigated the following displacement ranges $x = y = -0.1 \cdots 0.1$ m. This analysis pointed out that the calculation should be split in three areas as a consequence of the discontinuity of the arctan function. These areas are defined as at the left side ($x < -a$), covering ($-a < x < a$) and at the right side ($x > a$). Fig. 4 describes the case where the integration over the second conductor has to be split in three parts because the second conductor covers all the regions. The arctan function in eq. (9) fails at $x = -a$ and $x = a$ due a denominator becoming zero and a jump in the function value. The force is computed correctly when $|x| = a$ is excluded and the calculation is done per area. Consequently holds as maximum allowed value for region *I*: $x = -a(1 + \varepsilon)$, for region *II*: $-a(1 - \varepsilon) < x < a(1 - \varepsilon)$ and for region *III*: $x > a(1 + \varepsilon)$. The total force is then obtained summing the separate contributions. The value of ε is mainly determined by the accuracy of the machine accuracy; the value used here is 10^{-4}. The position and width of the second conductor determines whether the calculation has to be split in 1, 2 or 3 parts.

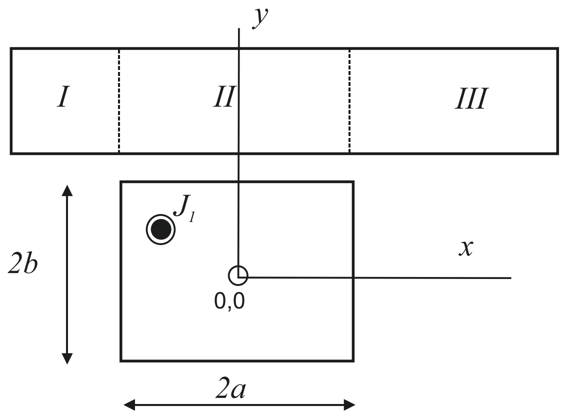

Fig. 4, graphical description of a case where the integration over the second conductor has to be split in three parts.

Here after one obtains Fig. 5 and 6 for the forces. The lack of a force level near the center is because the conductors cannot overlap each other. The error (Fig. 7) becomes in the order 10^{-6} or even more most likely as a consequence of the numerical inaccuracy of the double integration. This is the weak point when one is forced to use a numerical method because alternative methods allowing any combination of *x, y, a, b, A* and *B* are not found. Nevertheless, the noisy character and absence of tendencies over the *xy*-plane give rise to a growing confidence.

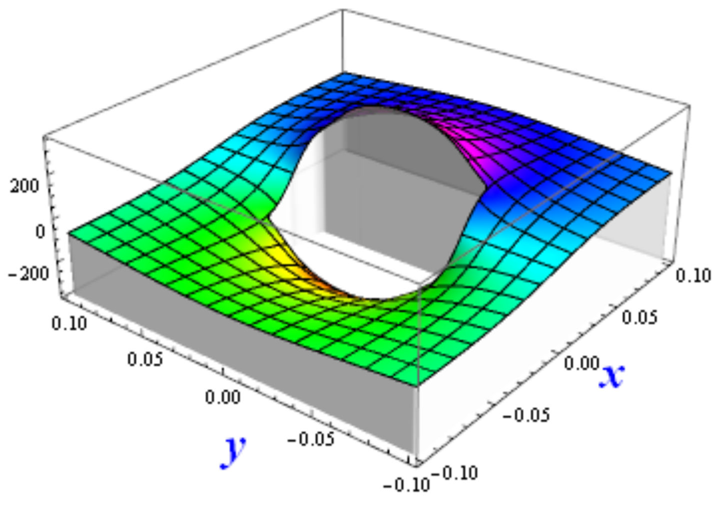

Fig. 5, force component F_x expressed in N/m.

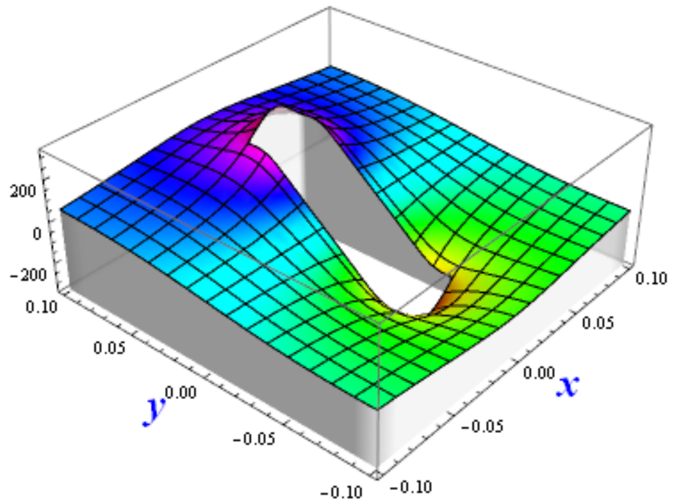

Fig. 6, force component F_y expressed in N/m.

The absolute difference between the analytically obtained Fig. 5 and the numerically integrated eq. (8) is presented by Fig. 7.

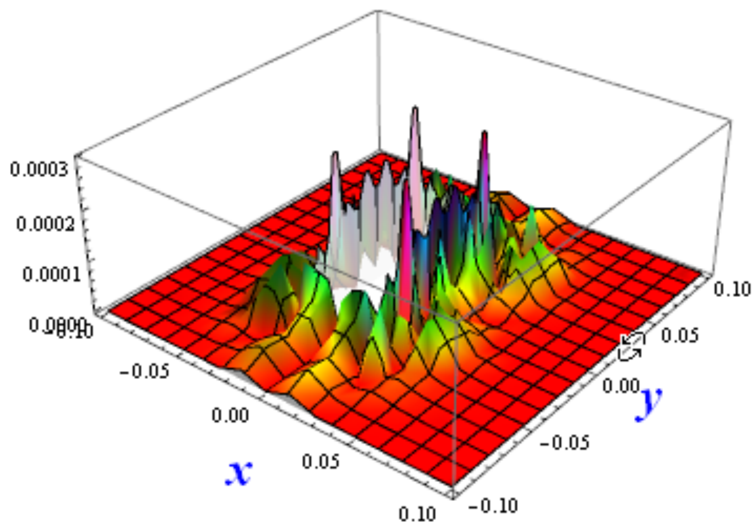

Fig. 7, difference numerical integrated eq. (8) versus eq. (10) expressed in N/m.

C. Comparison with Lit (Canova and Giaccone, 2009)

Lit. (Canova and Giaccone, 2009) offers an alternative, although we have to accept the same cross section for both conductors, $a = A = 0.01$ m, $b = B = 0.04$ m. The method described in (Canova and Giaccone, 2009) does not allow the alignment of conductor sides, so we can only investigate $x > 2A$ and $y > 2B$ with Fig. 8 as result. Rarely one needs a better level of agreement.

The noisy character and the absence of a significant tendency makes it likely that numerical calculation accuracy has to be considered as the cause of deviation.

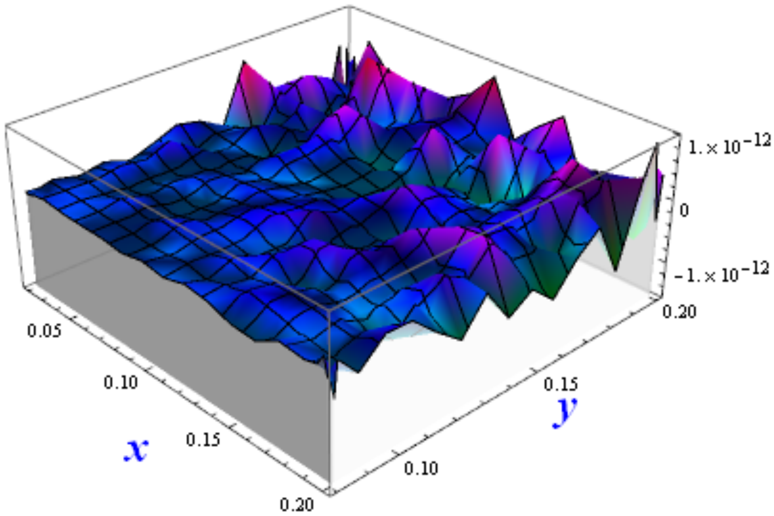

Fig. 8, relative deviation Lit.[2] versus eq. (10) expressed in N/m.

D. Comparison with 2D-FEM

2D-FEM makes it possible to apply different dimensions for the cross section of the bars. The program used is FEMM (Meeker, 2013), open boundary conditions have been used to minimize the effect of the domain truncation (Freeman and Lowther, 1988; Lowther et al., 1989). Fig. 9 shows the results and difference between (10) and the FEA results with as input, $a = A = 0.01$ m, b=0.04 m, B=0.01 m and $J_1 = J_2 = 10^7 \mathrm{A/m^2}$.

The differences found are less than 0.25% of the maximum force amplitude within the investigated *xy*-range. This result is considered by the authors as a confirmation of the correctness of (10) given the noisy character and the small differences. Finally, it is obvious that the proposed analytical method is faster than the other numerical techniques used for comparison. To quantify this aspect we refer to the results of Fig. 9. The analytical method provides the results in 3 seconds. The same results are obtained by means of FEMM in 43 minutes.

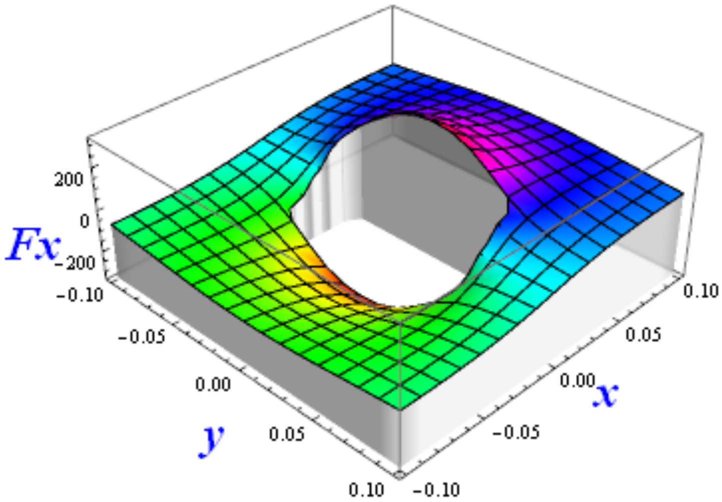

Fig. 9, analytical result for force component Fx expressed in N/m, according to eq. (9).

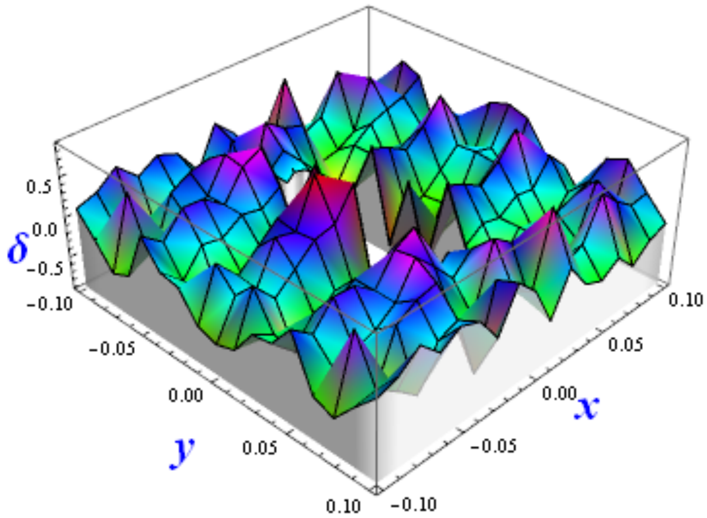

Fig. 10, difference between analytical result and FEA. Results expressed in N/m.

V. CONCLUSION

New equations for the forces between two rectangular bars, infinitely long, with a uniform current density are defined, compared with earlier results and verified. The profits in comparison to earlier publications are compactness and the options of different cross sections.

VI. APPENDIX 1

The force between two round conductors, infinitely long and carrying the currents I_0 and I becomes less straight forward when the finite cross sections are taken into account.

The straightforward rule per unit length gives as force:

$$F_o(d) = \mu_0 I_0 I/(2\pi d) \qquad \text{A1.1}$$

The current in the first conductor equals I_0 the center to center distance between the conductors equals *d* and the second conductor carries the current *I* and its radius is *R*. It is assumed that there is no overlap between the conductors.

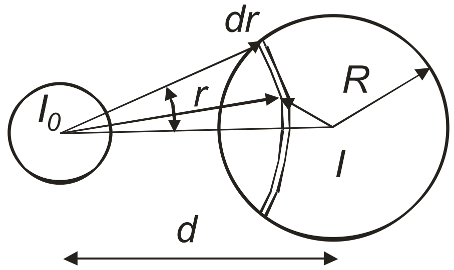

Fig. A.1.1, two round conductors.

The integral to be solved, based on the law of Lorentz, becomes:

$$F(d) = \int_{d-R}^{d+R} \int_{-\varphi}^{\varphi} B\, J\, r d\varphi dr = \int_{d-R}^{d+R} \int_{-\varphi}^{\varphi} \frac{\mu_0 I_0}{2\pi r} \frac{I}{\pi R^2} r\, d\varphi dr. \qquad \text{A.1.2}$$

The cosine-rule yields:

$$\varphi = \arccos\left(\frac{d^2 + r^2 - R^2}{2rd}\right). \qquad \text{A.1.3}$$

Substitution and use of the symbolic solver of Mathematica (Wolfram, 2012):

$$F(d) = 2 \int_{d-R}^{d+R} \frac{\mu_0 I_0}{2\pi} \frac{I}{\pi R^2} \arccos\left(\frac{d^2 + r^2 - R^2}{2rd}\right) dr \qquad \text{A.1.4}$$

$$= \frac{\mu_0 I_0}{2\pi} \frac{I}{\pi R^2} \left[\, r \arccos(u) + i \left\{(d - r)\mathrm{E}\big(i \operatorname{arcsinh}(v|w)\big) + 2\, R\, \mathrm{F}(v|w)\right\}\right]_{d-R}^{d+R}$$

, with $u(r) = \frac{d^2+r^2-R^2}{2rd}$, $v(r) = \sqrt{\frac{-r^2}{(d+R)^2}}$, $w = \frac{(d+R)^2}{(d-R)^2}$ and the two incomplete elliptic integrals, E and F as described by (Abramowitz, 1972). Substitution of the integration boundaries and further simplification yields:

$$F(d) = \frac{\mu_0 I_0 I}{\pi^2 R^2} \mathrm{Im}\left[(d-R)\left\{\mathrm{E}(w) - \mathrm{E}\left(\arcsin\left(\frac{1}{\sqrt{w}}\right)\middle|w\right)\right\} - 2\,R\,\left\{\mathrm{F}\left(\arcsin\left(\frac{1}{\sqrt{w}}\right)\middle|w\right) + \mathrm{F}\left(\frac{\pi}{2}\middle|w\right)\right\}\right] \quad \text{A.1.5}$$

$$= \frac{\mu_0 I_0 I}{\pi^2 R^2} \mathrm{Im}\left[(d+R)\mathrm{E}\left(\arcsin(\sqrt{w})\middle|\frac{1}{w}\right) - 2\,R\,\mathrm{F}\left(\arcsin(\sqrt{w})\middle|\frac{1}{w}\right)\right].$$

Using $I_0 = I = 1\,A$ and $R = 0.01\,m$ leads to Fig. A.1.2. The deviation of the straight forward rule for the force between conductors is obtained with the introduction of:

$$\Delta(d) = \frac{F(d)}{\mu_0 I_0 I/(2\pi d)}. \quad \text{A.1.6}$$

The result is given in Fig. A1.3 and it clearly shows that the validity of the simple rule is lost for $d < 5R$. The most extreme situation requires an infinitely thin conductor on the left side in Fig. A.1.1. and leads at *d/R*=1 to about 25% more force when *d/R*=1.

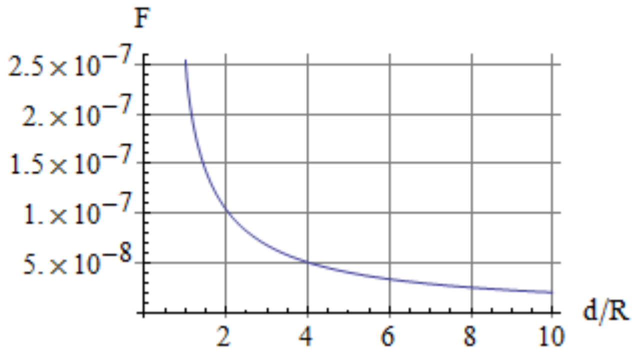

Fig. A.1.2, force *F(d)* in N versus *d/R*

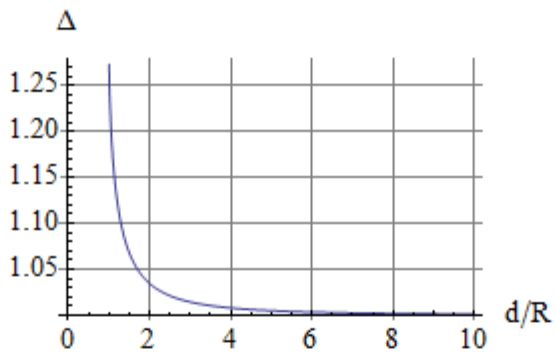

Fig. A.1.3, deviation Δ versus *d/R*

VII. APPENDIX 2

The following typographical errors were found during this study in (Canova and Giaccone, 2009):

$$S = 8b^3 - 12b^2 \rightarrow S = 8b^3 - 12b^2 h \quad \text{A.2.1}$$

$T = 8b^3 + 12b^2 \rightarrow T = 8b^3 + 12b^2h$ A.2.2

$F_x = \cdots 4h(I + G)\arctan\left(\frac{C}{H}\right) \rightarrow \ldots 4h(I + G)\arctan\left(\frac{C}{h}\right).$ A.2.3

REFERENCES

Abramowitz, M., I.A. Stegun, "*Handbook of Mathematical Functions*", Dover Publications, 1972, ISBN 0486-61272-4

Akoun, G., J.P. Yonnet, "3D analytical calculation of the forces exerted between two cuboidal magnets", *IEEE Trans. Magn.*, Vol. 20, No. 5, pp. 1962-1964, 1984.

Babic, S. I., C. Akyel, "Magnetic force calculation between thin coaxial circular coils in air", *IEEE Trans. Magn.*, Vol. 44, No. 4, pp. 445-452, 2008.

Binns, K.J., P.J. Lawrenson, C.W. Trowbridge, *The analytical and numerical solutions of electric and magnetic fields*, Wiley, pg. 71, ISBN 047192460-1

Canova, A., L. Giaccone, "Numerical and Analytical Modeling of Busbar Systems", *IEEE Trans Power Delivery*, vol. 24, No. 3, pp. 1568-1578, 2009

Compter, J. C., "Electro-dynamic planar motor," *Precision Eng*., vol. 28, No. 2, pp. 171-180, Apr. 2004

Dwight, H.B., "Repulsion between strap conductors", *Elec. World*, vol. 70, pp. 522-4, 1917

Freeman E. M., Lowther D. A., "A novel mapping technique for open boundary finite element solutions to Poissons equation", *IEEE Trans. Magn.*, Vol. 24, No. 6, pp. 2934-2936, 1988.

Giaccone L., Canova A., "Errata and comments for Numerical and analytical modeling of busbar systems", arXiv:1410.4056 [math.NA]

Haas, H., "Kräfte zwischen koaxialen Zylinderspulen", Archiv für Elektrotechnik 58, pp. 15-26, 1976.

Hammond, P., "The role of the potentials in electromagnetism", *Compel*, Vol. 18, No. 2, 103-119, 2015

Lowther D. A., Freeman E. M., Forghani B., "A sparse matrix open boundary method for finite element analysis", *IEEE Trans. Magn.*, Vol. 25, No. 4, pp. 2810-2812, 19889.

Meeker, D,.C., Finite Element Method Magnetics (FEMM), Version 4.2 (15 Nov 2013 Build), http://www.femm.info

Pissanetzky, S., Xiang, Y., “Analytical expressions for the magnetic field of practical coils”, *Compel*, Vol. 9, No. 2, 117-121, 1990

Ravaud, R., G. Lemarquand, V. Lemarquand, S. Babic, and C. Akyel, “Calculation of the magnetic field created by a thick coil," *Journal of Electromagnetic Waves and Applications*, Vol. 24, No. 10, pp. 1405-1418, 2010.

Ravaud, R., G. Lemarquand, V. Lemarquand, “Coils and Magnets: 3D Analytical Models, Piers Proceedings, Marrakesh, Morocco, pp. 1178-1184, 2011.

Rosser, W.G.V., *Interpretation of Classical Electromagnetism*, Kluwer Academic Publishers, pg. 30-31, ISBN 0-7923-4187-2

Rovers, J. M. M., J.W. Jansen, E.A. Lomonova, “Analytical calculation of the force between a rectangular coil and a cuboidal magnet”, *IEEE Trans. Magn.*, Vol. 46, No. 6, pp. 1656-1959, 2010.
Pissanetzky, S., Xiang, Y., “Analytical expressions for the magnetic field of practical coils”, *Compel*, Vol. 9, No. 2, 117-121, 1990
Urankar, Laxmikant K., “Vector potential and magnetic field of current-carrying finite arc segment in analytical form, Part III: Exact computation for rectangular cross section”*, IEEE Trans Magn.,* Vol. 18, No. 6, pp.1860-1867, 1982

Wolfram Research Europe Ltd, Mathematica version 9.0 (2012), Oxfordshire, UK